# Whole-Exome Sequencing Identifies Mutations of *KIF22* in Spondyloepimetaphyseal Dysplasia with Joint Laxity, Leptodactylic Type

Byung-Joo Min,[1,9] Namshin Kim,[3,9] Taesu Chung,[4] Ok-Hwa Kim,[5] Gen Nishimura,[6] Chin Youb Chung,[2] Hae Ryong Song,[7] Hyun Woo Kim,[8] Hye Ran Lee,[2] Jiwoong Kim,[3] Tae-Hoon Kang,[1] Myung-Eui Seo,[1] San-Deok Yang,[1] Do-Hwan Kim,[1] Seung-Bok Lee,[1] Jong-Il Kim,[1] Jeong-Sun Seo,[1] Ji-Yeob Choi,[1] Daehee Kang,[1] Dongsup Kim,[4] Woong-Yang Park,[1,*] and Tae-Joon Cho[2,*]

Spondyloepimetaphyseal dysplasia with joint laxity (SEMDJL), leptodactylic (lepto-SEMDJL) or Hall type, is an autosomal-dominant skeletal dysplasia manifesting with short stature, joint laxity with dislocation(s), limb malalignment, and spinal deformity. Its causative gene mutation has not yet been discovered. We captured and sequenced the exomes of eight affected individuals in six unrelated kindreds (three individuals in a family and five simplex individuals). Five novel sequence variants in *KIF22*, which encodes a member of the kinesin-like protein family, were identified in seven individuals. Sanger sequencing of *KIF22* confirmed that c.443C>T (p.Pro148Ser) cosegregated with the phenotype in the affected individuals in the family; c.442C>T (p.Pro148Leu) or c.446G>A (p.Arg149Gln) was present in four of five simplex individuals, but was absent in unaffected individuals in their family and 505 normal cohorts. *KIF22* mRNA was detected in human bone, cartilage, joint capsule, ligament, skin, and primary cultured chondrocytes. In silico analysis of KIF22 protein structure indicates that Pro148 and Arg149 are important in maintaining hydrogen bonds in the ATP binding and motor domains of KIF22. We conclude that these mutations in *KIF22* cause lepto-SEMDJL.

Spondyloepimetaphyseal dysplasia with joint laxity (SEMDJL), leptodactylic (lepto-SEMDJL) or Hall type (MIM 603546), is a rare but distinct entity of the spondyloepimetaphyseal dysplasias group. Hall et al.[1] first described this disease entity in 1998, differentiating it from spondylar and nasal alterations with striated metaphyses (SPONASTRIME) dysplasia (MIM 271510) and SEMDJL, Beighton type (MIM 271640). Since then, several series of affected individuals have been reported.[2–8] Subsequently, the nosology was confirmed as lepto-SEMDJL or SEMDJL Hall type.[9,10] It is considered an autosomal-dominant or possibly X-linked dominant trait on the basis of studies of three families in which it was inherited either from mother to son and/or daughter[6,7] or from father to daughter.[3]

Lepto-SEMDJL is characterized by short stature, distinctive midface retrusion, progressive knee malalignment (genu valgum and/or genu varum), generalized ligamentous laxity, and mild spine deformity, but intellectual development is not impaired.[1,5–7] Radiographic characteristics include significantly retarded epiphyseal ossification that evolves into epiphyseal dysplasia and precocious osteoarthritis, metaphyseal irregularities and vertical striations, constricted femur neck, slender metacarpals/metatarsals, and mild thoracolumbar kyphosis or scoliosis with normal or mild platyspondyly[5,7](Figure 1).

This study was approved by the institutional review boards of the participating institutions, and informed consent was obtained from all subjects. We performed genomic analysis on three affected individuals and an unaffected father from one family (Figure 2) and on five simplex individuals with lepto-SEMDJL to identify the disease-causing mutations. All subjects were of Korean origin and clinical and radiographic findings of five individuals were reported previously.[7] An additional three individuals were included in this study and clinical features of the eight affected individuals are summarized in Table 1. They all fulfilled the diagnostic criteria for lepto-SEMDJL on the basis of skeletal survey.

We first screened by using a high-resolution microarray (SurePrint G3 Human CGH Microarray Kit, 1X1M, Agilent Technologies, Santa Clara, CA), which did not reveal any pathogenic copy-number variations at 2.1 kb overall median probe spacing in all affected individuals. We then performed whole-exome sequencing of eight affected individuals and the unaffected father of the familial case. The exome was captured with the Agilent SureSelect Human All Exon Kit covering 38 Mb (Agilent, Santa Clara, CA) and sequenced with the Illumina Genome Analyzer II platform (Illumina, San Diego, CA). We obtained a mean coverage depth of the exome ranging from 39.5× to 60.8×, which is of sufficient depth to

[1]Department of Biomedical Sciences, Seoul National University College of Medicine, Seoul 110-799, Korea; [2]Department of Orthopaedic Surgery, Seoul National University College of Medicine, Seoul 110-799, Korea; [3]Korean Bioinformation Center, Korea Research Institute of Bioscience and Biotechnology, Daejeon 305-806, Korea; [4]Department of Bio and Brain Engineering, Korea Advanced Institute of Science and Technology, Daejeon 305-701, Korea; [5]Department of Radiology, Ajou University Hospital, Suwon, Kyunggi 443-721, Korea; [6]Department of Pediatric Imaging, Tokyo Metropolitan Children's Medical Center, Kiyose, Tokyo 204-8567, Japan; [7]Department of Orthopaedic Surgery, Korea University Guro Hospital, Seoul 152-703, Korea; [8]Department of Orthopaedic Surgery, Yonsei University Severance Children's Hospital, Seoul 120-752, Korea
[9]These two authors contributed equally
*Correspondence: wypark@snu.ac.kr (W.-Y.P.), tjcho@snu.ac.kr (T.-J.C.)
DOI 10.1016/j.ajhg.2011.10.015. 

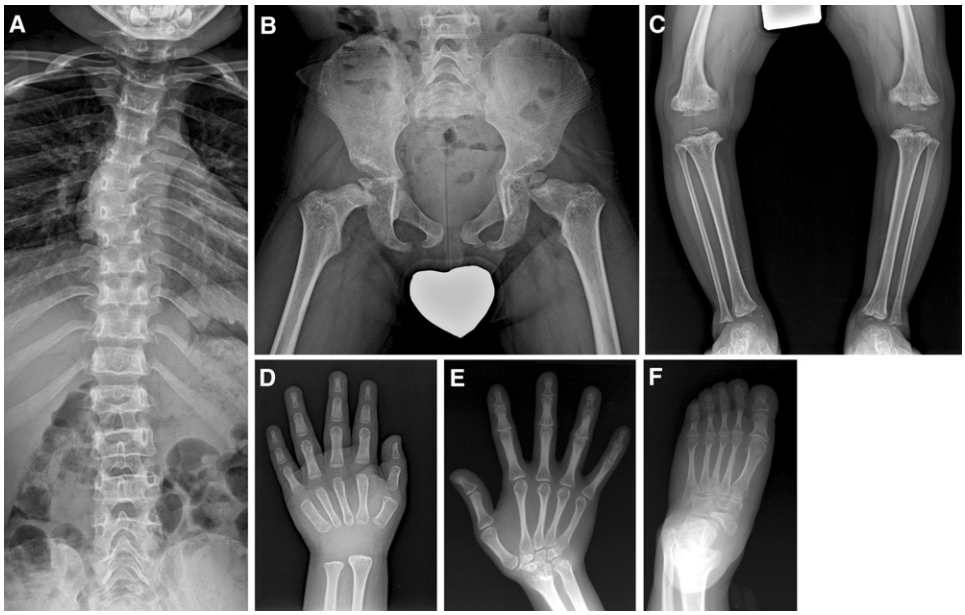


**Figure 1. Radiographic Characteristics of Lepto-SEMDJL**
(A–D) Spine, pelvis, knee, and hand of individual S-1 at age 4 show epimetaphyseal dysplasias with constricted femur neck, metaphyseal vertical streaks at the knee and ankle, genu varum deformity, and mild platyspondyly with thoracic scoliosis. Nonossified epiphyseal ossifications at the phalanges and carpal bones suggest remarkably retarded bone age.
(E and F) Hand and foot of individual F-1 (II-5 in Figure 2) at age of 45 show persistently slender metacarpals and metatarsals. Carpal and tarsal bones are small and dysplastic.

interrogate the exons for mutations (Table S1, available online).

Alignment of the affected individual sequences was performed with Burrows Wheeler Aligner[11] and Samtools[12]. Regions near short indels were realigned with IndelRealigner function in Genome Analysis Toolkit[13] with default parameters. Single nucleotide variants (SNVs) and indels affecting coding sequence or splicing sites were identified with Unified Genotype and annotated by Genomic Annotator.[14] All genomic changes were filtered against of dbSNP (build 132), 1000 Genomes Project (February 28, 2011, releases for SNVs, February 16, 2011, release for indels), and 18 genomes from healthy ethnic Korean individuals.[15]

A total of 5.1 Gb sequence mapped uniquely per individual as paired-end 76 bp reads to the human reference genome. More than 97% of the targeted bases were covered

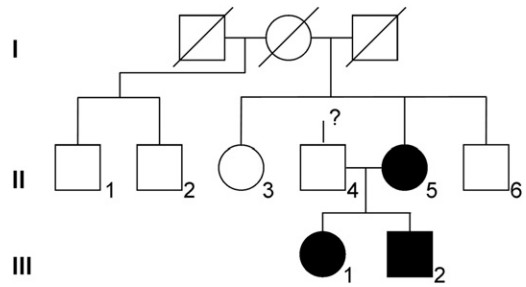


**Figure 2. Pedigree of the Familial Case**
Symbols in black indicate affected individuals.

to pass our thresholds for variant calling at this depth of coverage (Table S1). In the familial case, 97 novel candidate variants in 86 genes were inherited from the mother to the two affected offspring (Figure 2 and Table S1). Next, we sought to discover any gene with recurrent mutations between the family and the five simplex individuals. Surprisingly, *KIF22* (KINESIN family member 22 [MIM 603213]) was found to harbor sequence variants in seven of eight affected individuals, including three known SNPs (rs67578835, rs235648, and rs2450399) and five novel variants (Figure 3 and Table 2). All 14 exons and their flanking intron sequences of *KIF22* were amplified for Sanger sequencing from genomic DNA of the eight affected individuals, nine unaffected family members, and 505 healthy Korean individuals (Table S2 for primers sequence). Of five novel sequence variants, c.695G>A (p.Arg232Gln) in individual S-3 and c.1677+124A>T in individual S-4 were considered as polymorphisms because they were inherited from unaffected mothers (Table 2), and the latter was also found at a low frequency in the normal Korean cohort database (Table S3).

One of the three novel heterozygous sequence variations at residues Pro148 or Arg149 was found in the three affected individuals of the familial case and four of five simplex individuals and not in 1,010 control chromosomes from normal cohorts. The sequence variation, c.442C>T (p.Pro148Ser) cosegregated with the phenotype in the familial case. The sequence variations c.446G>A (p.Arg149Gln) in individual S-1 and c.443C>T (p.Pro148Leu) in individuals S-4 and S-5 were results of

**Table 1. Clinical Summary of the Patients**

| | Familial Cases | | | Simplex Cases | | | | |
|---|---|---|---|---|---|---|---|---|
| | F-1 (II-5[a]) | F-2 (III-1[a]) | F-3(III-2[a]) | S-1 | S-2 | S-3 | S-4 | S-5 |
| **Gender** | **F** | **F** | **M** | **M** | **M** | **F** | **F** | **F** |
| **Height** | | | | | | | | |
| Age of examination (in years) | 45 | 11 | 8 | 4 | 13 | 12 | 4 | 13 |
| Z value | −9.2 | −4.9 | −4.4 | −3.0 | −1.7 | −3.2 | −4.2 | −5.3 |
| Birth weight (kg) | (low) | 2.0 | 2.75 | 2.91 | 2.8 | 3.3 | 2.9 | 3.3 |
| **Clinical Findings** | | | | | | | | |
| Midface retrusion | obvious | obvious | obvious | obvious | mild | mild | obvious | obvious |
| Radial head (sub)luxation | yes | yes | yes | yes | no[b] | no[c] | yes | yes |
| Knee | genu valgum, bilateral | genu varum, bilateral | genu valgum, bilateral | genu varum, bilateral | genu valgum with patellar dislocation, bilateral | genu valgum, right > left | windswept deformity | genu varum, mild |
| Hip | dislocation, right | none | none | none | none | none | subluxation, right | none |
| Spine deformity | scoliosis | none | none | kyphoscoliosis, mild | none | scoliosis, mild | kyphosis, mild | mild kyphosis, resolved |
| Laryngotracheomalacia | yes | yes | yes | yes | denied | denied | yes | denied |
| Other | | | strabismus | | | | | epilepsy[d] |
| Individual numbering in Kim et al.[7] | 2 | 3 | 1 | new | new | 4 | new | 6 |

[a] In Figure 2.
[b] Cubitus varus with elbow flexion contracture.
[c] Mild flattening of the capitellum only.
[d] Benign Rolandic epilepsy, controlled by medication.

de novo mutation (Table 2). We therefore conclude that these sequence variants in *KIF22* are the strongest candidate mutations for autosomal-dominant lepto-SEMDJL (Table S3).

The mouse *Kif22* is expressed in various tissues including thymus, spleen, testis, and fetal liver[16]. Because lepto-SEMDJL involves primarily the connective tissues, we examined the expression of *Kif22/KIF22* in various tissues, including bone and cartilage, of mouse and human by RT-PCR with gene-specific primers (Table S2). In C57BL mice, *Kif22* mRNA was expressed in bone, cartilage, liver, ovary, small intestine, and spleen (Figure S1A). *KIF22* mRNA was detected in bone, cartilage, joint capsule, ligament, skin, and primary cultured chondrocytes harvested from human donors (Figure S1B).

Kinesin binds to ATP and hydrolyzes it to provide energy for molecular motors, and many regions in kinesin are involved in ATP binding.[17] Although a crystal structure of KIF22 (Protein Data Bank number 3BFN) is available, there are many missing structural parts, including one α-helix (from sequence number 231 to 241, NRTVGATRLNQ) that is known to be critical to ATP binding.[17] An additional reference structure, (3KIN, a homodimer structure for kinesin motor and neck domain with bound ADP) was selected to predict the structures of missing α-helix part in KIF22 with MODELER[18] (Figure S2A). The amino acid substitutions were applied to the modeled structure and the side chains of the mutated residues were optimized with FoldX,[19] and the structural changes due to the mutations were investigated by the molecular dynamics (MD) simulations with GROMACS.[20] Structural analysis and visualization were performed with PyMOL.[21]

A helix-loop-helix structure adjacent to the ATP binding site spans from129 to 156 amino acid residues containing Pro148 and Arg149 (Figure S2B). The loop structure adjacent to the ATP binding site is stabilized by hydrogen bonds among its residues, for example, Leu138 with Gly145, Pro144 with Ser140, and Gln143 and Glu142 with Ser140 as shown in Figure S1B. Loop residues also interact with the adjacent α-helix and other residues near the loop region; for example, Gln143 with His135 and Gly145 with Arg149.

In the MD simulation on the p.Pro148Leu mutation, we found two novel hydrogen bonds, which were absent in wild-type (Figures 4A and 4B). The hydrogen bond between NH of Arg149 and C = O of Gly145 is the expected regular hydrogen bond between $i^{th}$ and $(i+4)^{th}$

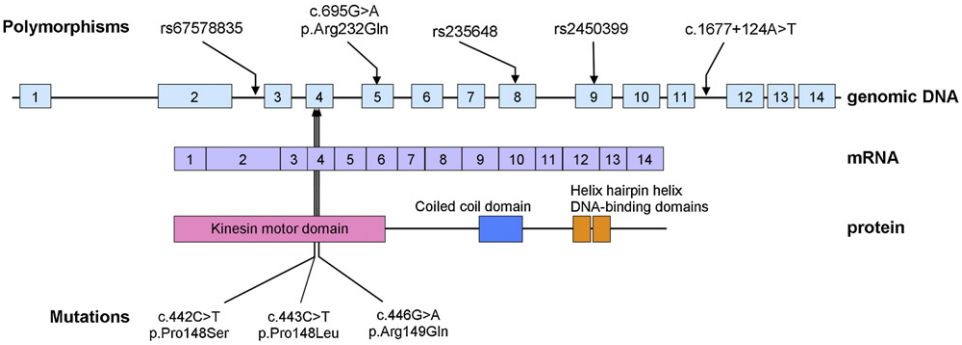


**Figure 3. KIF22 Mutations and Polymorphisms Identified in Individuals with Lepto-SEMDJL**
Three pathogenic variants of KIF22, p.Pro148Ser, p.Pro148Leu, and p.Arg149Gln, are located at the exon 4, substituting Pro148 or Arg149.

residues in the helix structure. The other hydrogen bond was formed between NH of Leu148 and C = O of Leu138. These two new hydrogen bonds slightly pull the loop structure away from ATP binding pocket, damaging ATP binding and probably resulting in the loss of motor function. We also obtained identical results for p.Pro148Ser.

With regard to the effect of the mutation, p.Arg149Gln, Arg149 forms a hydrogen bond with Gln101 and Tyr104 residues in an α-helix located near ATP binding site and also with the loop residue Pro144 (Figure 4C). The p.Arg149Gln mutation would disrupt the hydrogen bonds with the α-helix of Gln101 and Tyr104 (Figure 4D). Analogous to mutations in Pro148, the connection between two α-helices would be loosened to move away from the ATP binding pocket.

An α-helix spanning from 231 to 241 contains a sequence variation, p.Arg232Gln of individual S-3, which was considered as a polymorphism. Arg232 forms a hydrogen bond with residue Ser243 in an α-helical structure that is part of the ATP binding pocket (Figure S2C). Although the mutation p.Arg232Gln breaks a hydrogen bond between Arg149 and Ser242, it creates a new hydrogen bond between Gln232 and Arg242, maintaining proper interaction with the α-helix (Figure S2D), and hence does not seem to change the KIF22 structure significantly.

Although the role of KIF22 in humans is not thoroughly investigated, animal models with mutations in *KIF22* provide valuable information about the function of this gene. Xkid, a *Xenopus* ortholog of human KIF22, was degraded in anaphase by ubiquitin-mediated proteolysis, and degradation was necessary to support the chromosome movement at anaphase.[22,23] Loss of Xkid function in the stage of anaphase chromosome compaction resulted in the formation of multinucleated oocytes and embryonic death.[23] NOD, a *Drosophila* ortholog of KIF22, is required for the proper segregation of chromosomes. The role of KIF22 in the development of the skeletal system has not been elucidated yet. However, the formation of primary cilia, another key role for kinesin family proteins, could

**Table 2. Summary of Sequence Variations in *KIF22* in Lepto-SEMDJL Patients**

| | Familial Cases | | | Simplex Cases | | | | |
|---|---|---|---|---|---|---|---|---|
| **Individual** | **F-1 (II-5[a])** | **F-2 (III-1[a])** | **F-3 (III-2[a])** | **S-1** | **S-2** | **S-3** | **S-4** | **S-5** |
| **KIF22 Sequence Variants** | | | | | | | | |
| Mutation | c.442C>T (p.Pro148Ser) | c.442C>T (p.Pro148Ser) | c.442C>T (p.Pro148Ser) | c.446G>A (p.Arg149Gln) | none (none) | c.446G>A (p.Arg149Gln) | c.443C>T (p.Pro148Leu) | c.443C>T (p.Pro148Leu) |
| Polymorphism | rs235648 rs2450399 | rs235648 rs2450399 | rs235648 rs2450399 | rs235648 rs2450399 rs67578835 | rs235648 rs2450399 | c.695G>A (p.Arg232Gln) rs235648 rs2450399 | rs235648 rs2450399 c.1677+124>T | rs235648 rs2450399 |
| **Parental Genotypes** | | | | | | | | |
| Mother | n.a. | individual F-1 | individual F-1 | rs235648 rs2450399 rs67578835 | rs235648 rs2450399 rs67578835 | rs235648 rs2450399 c.695G>A (p.Arg232Gln) | rs235648 rs2450399 c.1677+124>T | rs235648 rs2450399 |
| Father | n.a. | rs235648 rs2450399 | rs235648 rs2450399 | rs235648 rs2450399 | n.a.[b] | n.a.[b] | rs235648 rs2450399 | rs235648 rs2450399 |

[a] In Figure 2.
[b] n.a. is used as an abbreviation for not available.

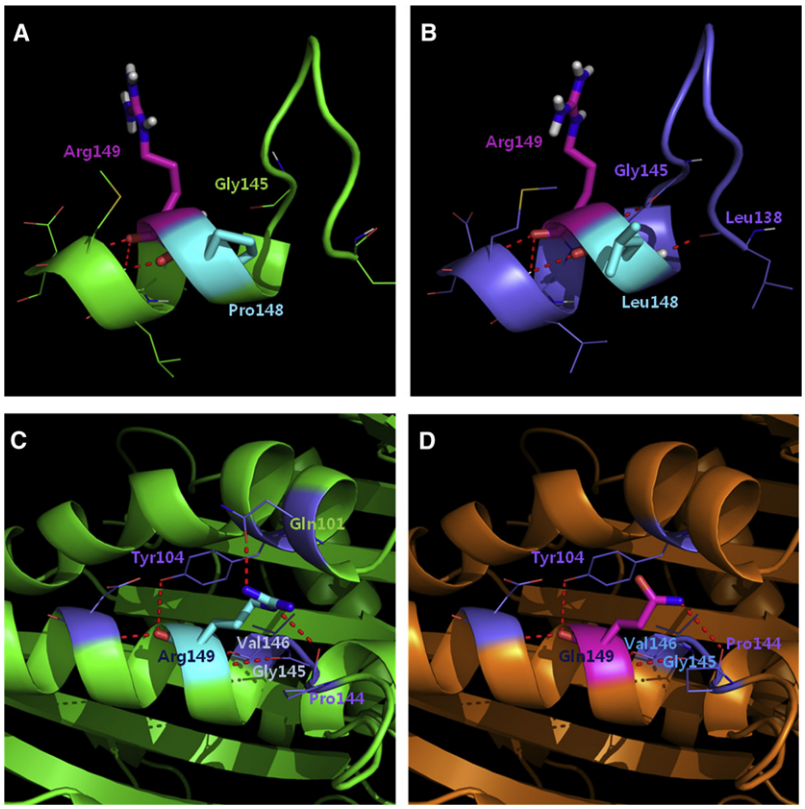


**Figure 4. 3D Structure of KIF22 and the Effect of Mutations**

(A) The wild-type structure was obtained by running MD simulation.

(B) The mutant structure with Pro148Leu mutation from MD simulation revealed two new hydrogen bonds; the hydrogen bond between NH of Arg148 and C = O of Gly145, and the hydrogen bond between NH of Leu148 and C = O of Leu138.

(C) Arg149 forms a hydrogen bond with Gln101 and Tyr104 residues in an α-helix located near ATP binding site and also with loop residue Pro144.

(D) The p.Arg149Gln mutation would disrupt the hydrogen bonds with the α-helix of Gln101 and Tyr104. The red dotted line symbolizes a hydrogen bond.

be crucial. Many members of the kinesin family control the formation of primary cilia, which deliver the signals from extracellular cues for development and tissue homeostasis. Kif3a,[24] Kif7,[25] and Kif24[26] support the formation of primary cilia in keratinocytes, retinal cells, and chondrocytes, respectively. Kif24, a kinesin-13 subfamily member, plays a role in regulating centriolar length and ciliogenesis. Loss of Kif24 from cycling cells resulted in aberrant cilia assembly but did not promote growth of abnormally long centrioles.[27] Mutations in *KIF7* were reported in human Joubert syndrome, and knockdown of *KIF7*(MIM 611254) caused problems in cilia formation, centrosomal duplication, and golgi network[25]. Knockout of Kif3a in the mouse resulted in depletion of cilia and postnatal dwarfism because of premature loss of the growth plate, probably a result of reduced proliferation and accelerated hypertrophic differentiation of chondrocytes.[28] Kif3a regulates important developmental processes such as skeletogenesis[28] and skin differentiation[26] through the formation of primary cilium. Their deficiency causes abnormal topography of hedgehog signaling, growth plate dysfunction, and nonphysiologic responses and processes in perichondrial tissues, including ectopic cartilage formation and excessive intramembranous ossification.[28] It is likely that the specific mutations of *KIF22* identified in individuals with lepto-SEMDJL could interfere with hedgehog signaling as in Kif3a knock-out mice resulting in osteochondrodysplasia phenotype.

We did not detect any mutation of *KIF22* in individual S-2 by either exome or Sanger sequencing, and no notable genomic imbalance greater than 2.1 kb was detected by aCGH analysis, either (data not shown). This individual showed a relatively mild clinical phenotype, including moderate short stature ($z = -1.7$ at age 13 years) and equivocal midface retrusion, suggesting the possibility of a mutation in another gene related to *KIF22*.

Given the mutations in *KIF22* identified in this cohort, the *KIF22* expression pattern in connective tissues, and the predicted protein structural changes caused by these mutations, we conclude that the specific mutations of *KIF22* affecting amino acid 148 or 149 are pathogenic for lepto-SEMDJL. The mechanism by which these mutations lead to disease is likely related to motor dysfunction of KIF22, but additional studies will be needed to elucidate the KIF22 function in the skeletal system and to understand the molecular pathogenesis of lepto-SEMDJL associated with *KIF22* mutation.

## Supplemental Data

Supplemental Data include two figures and three tables and can be found with this article online at http://www.cell.com/AJHG/.

## Acknowledgments

The authors deeply appreciate Andrea Superti-Furga and Sheila Unger for reviewing the affected individuals, Murim Choi and Charles Lee for reading the manuscript, and Soong Deok Lee for helping DNA preparation. This study was supported by a grant from the Korea Healthcare Technology Research and Development Project, Ministry for Health, Welfare and Family Affairs, Republic of Korea (No A080588).

Received: September 7, 2011
Revised: October 20, 2011
Accepted: October 31, 2011
Published online: December 8, 2011

## Web Resources

The URLs for data presented herein are as follows:

1000 Genomes Project (February 28, 2011 releases for SNPs, February 16, 2011 release for indels), http://www.1000genome.org

Consensus Coding Sequence Region (CCDS) database, http://www.ncbi.nlm.nih.gov/projects/CCDS/

GROMACS, http://www.gromacs.org

Online Mendelian Inheritance in Man (OMIM), http://www.omim.org

Pymol, http://www.pymol.org

UCSC database, version hg19 (NCBI Build 37, 1 Feb 2009), http://genome.ucsc.edu/

## Accession Numbers

Two novel polymorphisms detected in this study were registered to dbSNP as ss469414041 (c.695G>A, p.Arg232Gln) and ss469414042 (c.1677+124A > T). The three sequence variations considered pathogenic were registered to dbSNP, as ss475871913 (c.443C>T, p.Pro148Ser), ss475871912 (c.442C>T, p.Pro148Leu), and ss475871914 (c.446G>A, p.Arg149Gln).

## References


1. Hall, C.M., Elçioglu, N.H., and Shaw, D.G. (1998). A distinct form of spondyloepimetaphyseal dysplasia with multiple dislocations. J. Med. Genet. *35*, 566–572.
2. Rossi, M., De Brasi, D., Hall, C.M., Battagliese, A., Melis, D., Sebastio, G., and Andria, G. (2005). A new familial case of spondylo-epi-metaphyseal dysplasia with multiple dislocations Hall type (leptodactylic form). Clin. Dysmorphol. *14*, 13–18.
3. Hall, C.M., Elcioglu, N.H., MacDermot, K.D., Offiah, A.C., and Winter, R.M. (2002). Spondyloepimetaphyseal dysplasia with multiple dislocations (Hall type): Three further cases and evidence of autosomal dominant inheritance. J. Med. Genet. *39*, 666–670.
4. Mégarbané, A., Ghanem, I., and Le Merrer, M. (2003). Spondyloepimetaphyseal dysplasia with multiple dislocations, leptodactylic type: Report of a new patient and review of the literature. Am. J. Med. Genet. A. *122A*, 252–256.
5. Nishimura, G., Honma, T., Shiihara, T., Manabe, N., Nakajima, E., Adachi, M., Mikawa, M., Fukushima, Y., and Ikegawa, S. (2003). Spondyloepimetaphyseal dysplasia with joint laxity leptodactylic form: Clinical course and phenotypic variations in four patients. Am. J. Med. Genet. A. *117A*, 147–153.
6. Park, S.M., Hall, C.M., Gray, R., and Firth, H.V. (2007). Persistent upper airway obstruction is a diagnostic feature of spondyloepimetaphyseal dysplasia with multiple dislocations (Hall type) with further evidence for dominant inheritance. Am. J. Med. Genet. A. *143A*, 2024–2028.
7. Kim, O.H., Cho, T.J., Song, H.R., Chung, C.Y., Miyagawa, S., Nishimura, G., Superti-Furga, A., and Unger, S. (2009). A distinct form of spondyloepimetaphyseal dysplasia with joint laxity (SEMDJL)-leptodactylic type: Radiological characteristics in seven new patients. Skeletal Radiol. *38*, 803–811.
8. Holder-Espinasse, M., Fayoux, P., Morillon, S., Fourier, C., Dieux-Coeslier, A., Manouvrier-Hanu, S., Le Merrer, M., and Hall, C.M. (2004). Spondyloepimetaphyseal dysplasia (Hall type) with laryngeal stenosis: A new diagnostic feature? Clin. Dysmorphol. *13*, 133–135.
9. Superti-Furga, A., and Unger, S. (2007). Nosology and classification of genetic skeletal disorders: 2006 revision. Am. J. Med. Genet. A. *143*, 1–18.
10. Warman, M.L., Cormier-Daire, V., Hall, C., Krakow, D., Lachman, R., LeMerrer, M., Mortier, G., Mundlos, S., Nishimura, G., Rimoin, D.L., et al. (2011). Nosology and classification of genetic skeletal disorders: 2010 revision. Am. J. Med. Genet. A. *155A*, 943–968.
11. Li, H., and Durbin, R. (2009). Fast and accurate short read alignment with Burrows-Wheeler transform. Bioinformatics *25*, 1754–1760.
12. Li, H., Handsaker, B., Wysoker, A., Fennell, T., Ruan, J., Homer, N., Marth, G., Abecasis, G., and Durbin, R.; 1000 Genome Project Data Processing Subgroup. (2009). The Sequence Alignment/Map format and SAMtools. Bioinformatics *25*, 2078–2079.
13. McKenna, A., Hanna, M., Banks, E., Sivachenko, A., Cibulskis, K., Kernytsky, A., Garimella, K., Altshuler, D., Gabriel, S., Daly, M., and DePristo, M.A. (2010). The Genome Analysis Toolkit: A MapReduce framework for analyzing next-generation DNA sequencing data. Genome Res. *20*, 1297–1303.
14. Zanders, S., Ma, X., Roychoudhury, A., Hernandez, R.D., Demogines, A., Barker, B., Gu, Z., Bustamante, C.D., and Alani, E. (2010). Detection of heterozygous mutations in the genome of mismatch repair defective diploid yeast using a Bayesian approach. Genetics *186*, 493–503.
15. Ju, Y.S., Kim, J.I., Kim, S., Hong, D., Park, H., Shin, J.Y., Lee, S., Lee, W.C., Kim, S., Yu, S.B., et al. (2011). Extensive genomic and transcriptional diversity identified through massively parallel DNA and RNA sequencing of eighteen Korean individuals. Nat. Genet. *43*, 745–752.
16. Tokai, N., Fujimoto-Nishiyama, A., Toyoshima, Y., Yonemura, S., Tsukita, S., Inoue, J., and Yamamota, T. (1996). Kid, a novel kinesin-like DNA binding protein, is localized to chromosomes and the mitotic spindle. EMBO J. *15*, 457–467.
17. Kozielski, F., Sack, S., Marx, A., Thormählen, M., Schönbrunn, E., Biou, V., Thompson, A., Mandelkow, E.M., and Mandelkow, E. (1997). The crystal structure of dimeric kinesin and implications for microtubule-dependent motility. Cell *91*, 985–994.
18. Sali, A., and Blundell, T.L. (1993). Comparative protein modelling by satisfaction of spatial restraints. J. Mol. Biol. *234*, 779–815.
19. Schymkowitz, J., Borg, J., Stricher, F., Nys, R., Rousseau, F., and Serrano, L. (2005). The FoldX web server: An online force field. Nucleic Acids Res. *33* (Web Server issue), W382–W388.
20. Van Der Spoel, D., Lindahl, E., Hess, B., Groenhof, G., Mark, A.E., and Berendsen, H.J. (2005). GROMACS: Fast, flexible, and free. J. Comput. Chem. *26*, 1701–1718.
21. The PyMOL Molecular Graphics System, Version 1.3, Schrödinger, LLC.
22. Funabiki, H., and Murray, A.W. (2000). The Xenopus chromokinesin Xkid is essential for metaphase chromosome alignment and must be degraded to allow anaphase chromosome movement. Cell *102*, 411–424.
23. Ohsugi, M., Adachi, K., Horai, R., Kakuta, S., Sudo, K., Kotaki, H., Tokai-Nishizumi, N., Sagara, H., Iwakura, Y., and Yamamoto, T. (2008). Kid-mediated chromosome compaction ensures proper nuclear envelope formation. Cell *132*, 771–782.
24. Verhey, K.J., Kaul, N., and Soppina, V. (2011). Kinesin assembly and movement in cells. Annu Rev Biophys *40*, 267–288.

25. Dafinger, C., Liebau, M.C., Elsayed, S.M., Hellenbroich, Y., Boltshauser, E., Korenke, G.C., Fabretti, F., Janecke, A.R., Ebermann, I., Nürnberg, G., et al. (2011). Mutations in KIF7 link Joubert syndrome with Sonic Hedgehog signaling and microtubule dynamics. J. Clin. Invest. *121*, 2662–2667.

26. Ezratty, E.J., Stokes, N., Chai, S., Shah, A.S., Williams, S.E., and Fuchs, E. (2011). A role for the primary cilium in Notch signaling and epidermal differentiation during skin development. Cell *145*, 1129–1141.

27. Kobayashi, T., Tsang, W.Y., Li, J., Lane, W., and Dynlacht, B.D. (2011). Centriolar kinesin Kif24 interacts with CP110 to remodel microtubules and regulate ciliogenesis. Cell *145*, 914–925.

28. Koyama, E., Young, B., Nagayama, M., Shibukawa, Y., Enomoto-Iwamoto, M., Iwamoto, M., Maeda, Y., Lanske, B., Song, B., Serra, R., and Pacifici, M. (2007). Conditional Kif3a ablation causes abnormal hedgehog signaling topography, growth plate dysfunction, and excessive bone and cartilage formation during mouse skeletogenesis. Development *134*, 2159–2169.